International Society for Rock Mechanics and Rock Engineering
Macedonian Association for Geotechnics

ISRM Regional Symposium
Eurock 2026
Risk Management in Rock Engineering
Skopje, 15-19 September

DOI: https://doi.org/10.68732/c0058c211ebc9525
ISBN: 978-9989-2053-6-1

A new design method for load estimation in yielding tunnel linings

L. Batocchioni & E. Turrini
Sapienza University of Rome, Rome, Italy
lorenzo.batocchioni@uniroma1.it
0000-0003-0706-0826

C. Pandolfi
Polytechnic University of Turin, Turin, Italy

S. Miliziano
Geotechnical Design Group, Rome, Italy

Abstract

Designing yielding tunnel linings in squeezing ground requires an accurate evaluation of axial loads and bending moments from ground–lining interaction. While numerical modeling is computationally heavy and the Convergence-Confinement Method fails to capture internal force evolution, this study proposes a simplified analytical design method providing reliable first-order estimates to complement advanced tools. Based on charts derived from parametric analytical formulations, the method quantifies both the friction-induced axial load increment and the maximum bending moment caused by non-uniform stresses. This physically consistent approach ensures rapid, efficient screening across diverse ground conditions and lining configurations.

Keywords

Design methods, Tunnel lining, Yielding principle, Elasto-plastic elements, Analytical approaches.

1 Introduction

The growing demand for large underground infrastructure emphasizes the need to better understand ground-lining interaction (*GLI*) in deep tunnels, particularly under squeezing conditions (Barla 2001; Hoek 2001). In these cases, the yielding principle (*YP*) (Kovàri 1998) is the most effective design strategy. Implementing the *YP* typically involves adding Elasto-Plastic Elements (*EPEs*) to the temporary lining, allowing controlled circumferential deformation and stress relief through relative ground-lining movements. As projects become more complex, fast and reliable predictive tools are needed to estimate lining forces during preliminary design and to support numerical analyses.

In this context, developing methods to assess internal forces on tunnel support under the specific *GLI* of a yielding temporary lining is essential. When *EPEs* enter the yielding stage, the axial load is limited by the *EPEs*' yielding capacity and remains bounded, unlike in the rigid lining case. However, this comes with a significant bending moment (M_{EPE}), resulting from the support's heterogeneity and the localized concentration of ground normal stresses (σ_n) around the *EPEs*. Furthermore, shear stresses at the ground–lining interface, caused by friction during relative movements, partially increase axial load (ΔN_τ) while reducing the bending moment.

To overcome the limitations of the overly simplified Convergence–Confinement Method (Panet 1995) without relying on complex numerical analyses (Barla et al. 2011; Moritz 2011; Tian et al. 2016; Yang et al. 2023 and Batocchioni et al. 2024), which still require first-approximation input values, intermediate methodologies are needed. Radončić et al. (2009) proposed a semi-analytical formulation to estimate the axial load increment ΔN_τ; however, no method is currently available to evaluate the associated bending moment M_{EPE}. Batocchioni et al. (2026) introduced two semi-analytical approaches to assess (1) the bending moment arising from lining heterogeneities (M_{EPE}) and (2) the axial force increment induced by tangential stresses at the ground–lining interface (ΔN_τ). In the present paper, these methods are reformulated with a more practical focus, leading to two design abaci as the main outcome. Data from two well-documented case histories are finally presented for illustration.

2 Methodology

The proposed design method is based on a simplified analytical framework aimed at capturing the primary mechanics of ground–lining interaction in yielding supports. The formulation conceptualizes the lining as an assembly of rigid structural segments separated by deformable insert elements. The lining heterogeneity caused by the weak *EPEs* embedded in the rigid structural parts makes the *GLI* much more complex, as illustrated in the interaction diagrams in Fig. 1.

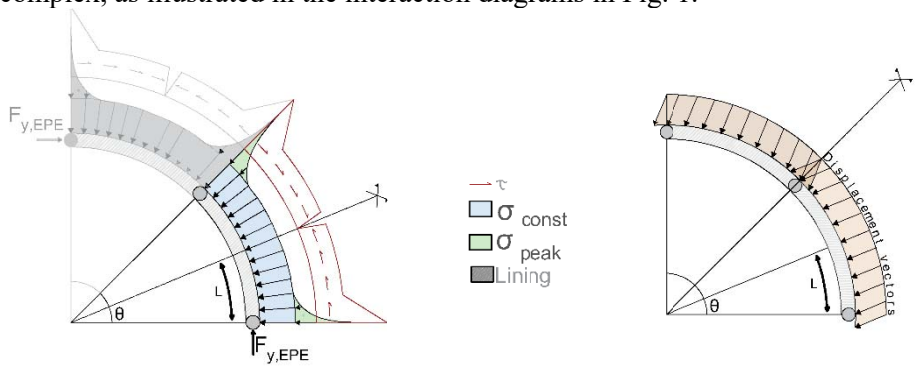


Fig. 1 Diagram of the ground–lining interaction: (left) loads from the ground (normal and shear stresses at the ground–lining interface) and (right) lining displacement vectors. The ground displacement vectors— not explicitly shown—are always radial; therefore, away from the midpoint, relative displacements at the interface are expected (see the shear stress direction).

The analysis focuses on the midpoint between two consecutive *EPEs* and on the adjacent boundaries. Stress concentration near the *EPEs* induces a bending moment at the midpoint (M_{EPE}), while ground–lining relative displacements generate shear stresses that oppose *EPE* closure and produce an axial load increment peaking at the midpoint (ΔN_τ). The proposed approach therefore evaluates internal forces at this critical section-the midpoint between two consecutive *EPEs*-for preliminary structural verification.The following semi-analytical procedures have been developed and validated via sensitivity analyses in (Batocchioni et al. 2026). Here for brevity, only the essential aspects will be reported.

A brief remark is required on the interface friction angle, a key parameter in *GLI* despite its limited physical meaning, as it condenses the complex interaction between steel sets, concrete shell, and ground into a single number. Its use is nevertheless standard in tunnelling and is therefore adopted here. For M_{EPE}, the effect of the interface shear stress (τ) is explicitly considered with a subtractive term, whereas for $\Delta N_\tau$the interface friction angle represents the governing input parameter.

$$M_{EPE} = M_{peak} - M_y = c_r F_y R(\theta sin\theta + cos\,\theta\ - 1) \tag{1}$$

The two semi-analytical equations obtained in Batocchioni et al. (2026) are:

Where c_r fraction of σ_n concentration near the *EPEs*, conservatively value equal to 0.2
F_y *EPEs* yield force
R tunnel radius
θ half of the angle between two consecutive *EPEs* (Fig. 1)

$$\Delta N_\tau = \int_0^{l/2} \tau \, dl = \frac{\mu F_y}{2} \frac{l}{R} \tag{2}$$

Where $\mu = tan(\varphi_{int}) = tan(\varphi - 10)$ interface friction coefficient
$l = \theta R$ half of arc length between two consecutive *EPEs* (Fig. 1) assuming $\sigma_n = const$

Eq. 1 is obtained by subtracting the bending moment induced by the concentrated normal stress at the rigid beam boundaries (M_{peak}, in Fig. 1 the green σ_{peak} are considered as a point load) from the opposing bending moment associated with *EPEs* yielding (M_y, caused by $F_{y,EPE}$). For the design abaci, Eq. 1 is then reformulated to homogenize the expressions. The angular coordinate θ is expressed in terms of the ratio between l and R, and the dependence on the soil friction angle ϕ is explicitly introduced by subtracting from M_{EPE} a second contribution due to interface shear stresses M_τ. Eq. 1, assuming $\sigma_n = const$ (in the new term) and $c_r = 0.2$, thus becomes:

$$M_{EPE} = M_{peak} - M_y - M_\tau = 0.2F_yR\left(\frac{l}{R}sin\frac{l}{R} + cos\frac{l}{R} - 1\right) - \mu F_yR\left(\frac{l}{R} - sin\frac{l}{R}\right) \tag{3}$$

Finally, Eq. 2 and Eq. 3 are used to construct the two design abaci, illustrated through selected tunnel sections from two well-known case histories: the Lyon-Turin Euralpin Tunnel (TELT, Bonini and Barla, 2012) and the Terzo Valicodei Giovi project (Batocchioni 2025).

3 Results

Fig. 2 presents the design abacus for the bending moment M_{EPE} as a function of the soil friction angle ϕ and the ratio l/R, which is conceptually equivalent to half of the angle between two consecutive *EPEs*. The values are generally conservative, as demonstrated in Batocchioni et al. (2026).

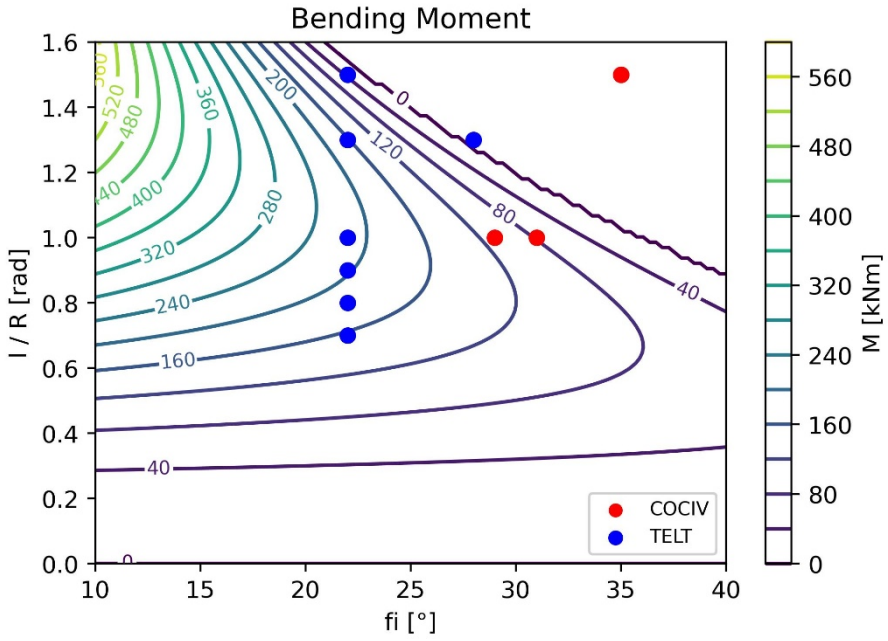


Fig. 2 Abacus for M_{EPE} in the ϕ–l/R domain. The values obtained are generally conservativeexceeding the actual value.

The abacus incorporates the frictional effect through the contribution of interface shear stresses. Neglecting this effect—and thus the subtractive term in Eq. 3—would result in M_{EPE} increasing mostly monotonically with l/R. Conversely, including this opposite contribution introduces a non-monotonic trend. While M_{EPE} generally grows with l/R due to wider *EPEs* spacing, an increase in both l/R and

ϕ simultaneously amplifies the two terms. At high values of l/R and ϕ, this reduction counteracts the growth of the bending moment. Consequently, the highest values of M_{EPE} are reached when large l/R is combined with low ϕ.

The case histories show that, particularly for the TELT project, the expected bending moment can be significant (up to 200 kNm), mainly due to the extensive use of highly spaced EPEs embedded in the lining with a not so frictional ground. Conversely, the points associated with the COCIV project fall in less critical regions of the abacus. Nevertheless, this indicates that, especially in cases such as TELT, simplified approaches should be complemented by more advanced analyses, such as numerical modelling, in order to more accurately assess the magnitude of the bending moment. In practice, when critical bending is anticipated, mitigation strategies involve optimizing the *EPEs* layout by reducing the spacing between consecutive elements-l. This adjustment also enhances the capacity to support ground loads. However, as the margin for further spacing reduction is typically narrow, a rigorous preliminary selection of the *EPEs* arrangement becomes essential.

The second abacus, shown in Fig. 3, presents the design abacus for the normalized axial load increment $\Delta N_\tau/F_y$ in the same ϕ –l/R plane adopted above. Unlike the bending moment, the axial increment increases monotonically with both ϕ and l/R. For a fixed ϕ, larger l/R ratios correspond to longer interaction lengths over which tangential stresses can accumulate, leading to higher axial force increments. Conversely, for a given ll/R, increasing ϕ enhances the shear transfer capacity at the soil–lining interface, resulting in a greater contribution of ΔN_τ. As shown in the abacus, low friction angles combined with short interaction lengths lead to negligible axial increments, whereas higher ϕ values acting over extended lining segments may generate normalized increments approaching 40%.

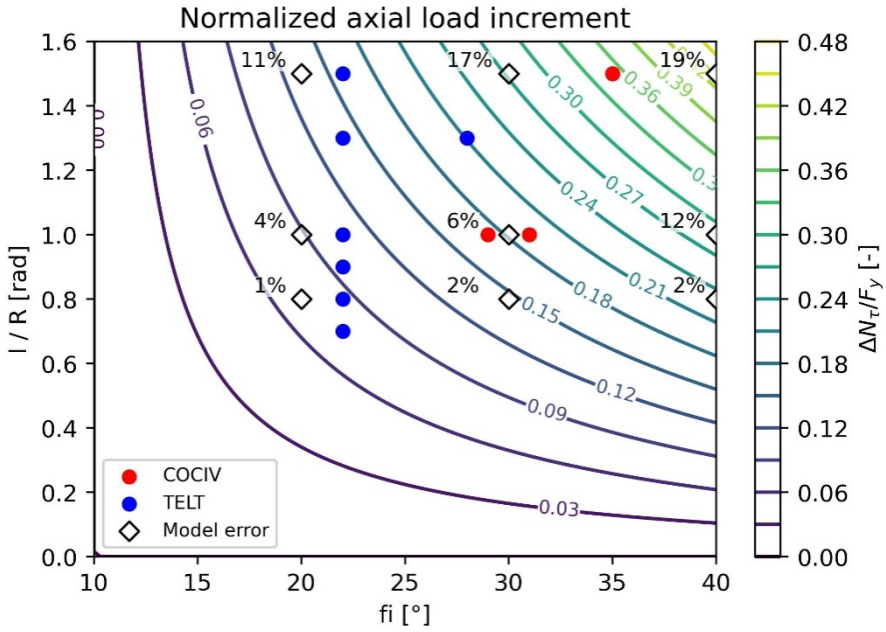


Fig. 3 Abacus for ΔN_τ in the ϕ–l/R domain. The axial load increment is presented as normalized with respect to the yielding resistance of the *EPEs* (F_y).

It should also be noted that the curves are derived using the simplified method proposed by Radončić et al. (2009), which generally underestimate the numerical results. For selected combinations of l/R and ϕ, numerical analyses (Batocchioni 2025) were therefore performed and compared with the analytical predictions to evaluate the corresponding percentage error. As shown in Fig. 3, the error increases with both l/R and ϕ. For the M_{EPE} abacus (Fig. 2), the error evaluation was not included since the simplified formulation was observed to generally overestimate the numerical results.

The case histories highlight distinct behaviours. For the TELT project, characterized by moderate ϕ and relatively high l/R values, the $\Delta N_\tau/F_y$ remains moderate (typically below 0.20), indicating a limited amplification of the structural axial force at yielding. In contrast, the COCIV cases, associated with higher ϕ and comparable l/R ratios, exhibit significantly higher $\Delta N_\tau/F_y$, in some instances exceeding 30% with a 19% of model error, reaching an overall increment values of about 50%.

These results have significant conceptual implications for preliminary design. At this stage, a yielding ratio r_y is typically defined as the ratio between the yielding resistance of the *EPEs* and the axial resistance of the lining. In practice, $r_y \approx 0.5$ is commonly adopted to ensure controlled activation of the *EPEs*. However, at the onset of *EPEs* yielding, the axial force in the lining is $F_y + \Delta N_\tau$, not simply F_y. Therefore, when $\Delta N_\tau / F_y$ assumes high values-such 50%, the axial demand transferred to the lining increases significantly, effectively reducing the admissible value of r_y and restricting the design space. In such cases, the axial increment may be mitigated by reducing the interaction length l (i.e., decreasing *EPEs* spacing) or a lower yielding resistance F_y may be selected for the EPEs, thus reducing the total axial force mobilized in the lining at the activation stage, at the cost of higher tunnel convergence or lining structural demand.

A combined reading of the abaci highlights a clear interaction between the two governing mechanisms. As shown in the "Structural Criticality Regions" map (Fig. 4), it indicates that low ϕproduce a bending-dominated response, while higher ϕ values shift the mechanism toward axial demand. Both actions increase with the l/R ratio: larger spacings between consecutive *EPEs* amplify bending and axial effects, whereas lower l/R values limit the structural demand. For l/R< 0.57, the structural demand remains limited. Conversely, for l/R> 0.57, good conditions are achieved only for specific ϕ. For simplicity, the boundaries of the critical areas are approximated by 3 linear equations.

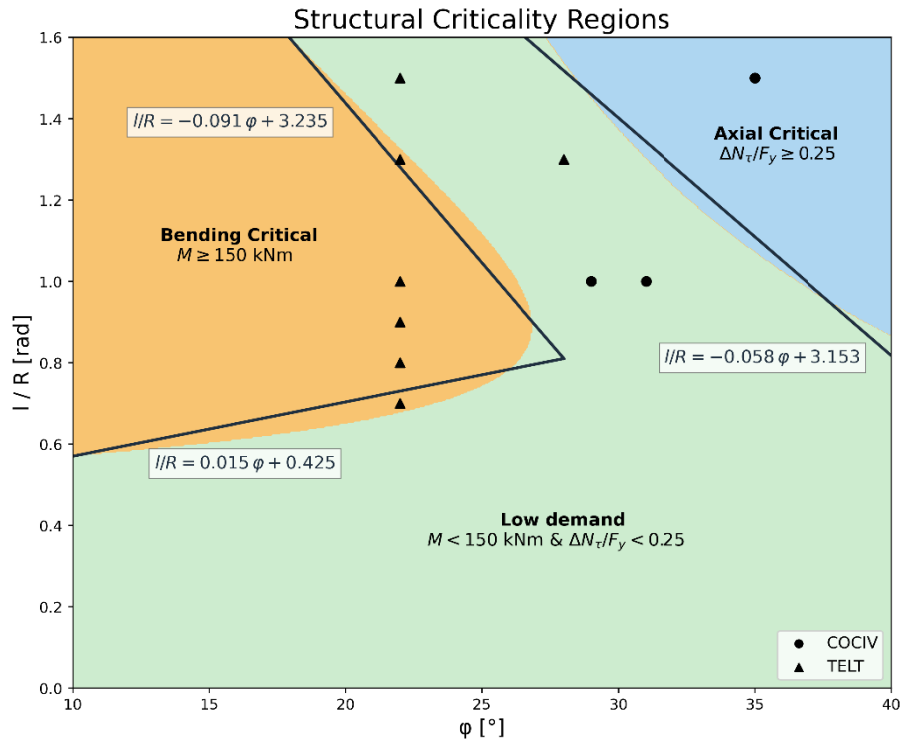


Fig. 4 Structural criticality map in the ϕ–l/R domain, showing bending-dominated, axial-dominated and low-demand regions defined by the adopted threshold. COCIV and TELT are superimposed to illustrate their position in the design space.

The resulting boundaries effectively summarize the application limits of the analytical method. This chart underscores how the optimization of *EPEs* spacing serves as a flexible design tool to safely navigate between bending- and axial-dominated structural risks before proceeding to advanced numerical modeling.

4 Conclusions

This study presents a simplified analytical approach for the preliminary assessment of internal forces in tunnel linings equipped with elasto-plastic elements. The method fills the gap between the Convergence-Confinement Method and numerical modeling by providing reliable first-order estimates of bending moments and normalized axial load increments.

Accordingly, two design abaci were developed to estimate: (i) the maximum bending moment induced by non-uniform ground stresses and (ii) the normalized axial load increment generated by interface shear transfer. The results highlight that while both axial forces and bending moments increase with wider elasto-plastic element spacing, axial demand is amplified by higher friction angles ($\phi > 30°$), whereas bending moments become more significant at lower values ($\phi < 20°$). These abaci serve as practical tools for preliminary design, providing a quick quantification of expected internal forces and a rational reference for subsequent numerical analyses.

Furthermore, a summary chart synthesizes these findings, identifying practical design ranges and the governing structural mechanisms. The analysis indicates that small elasto-plastic elements spacing ensures limited structural demand across all friction angles. Conversely, for larger spacings, acceptable conditions are restricted to intermediate friction angles, as extreme values (low or high) lead to bending- and axial-dominated responses, respectively.

Ultimately, elasto-plastic elements spacing emerges as the primary governing parameter for lining optimization-particularly since the soil friction angle is not a design parameter, but rather an inherent geotechnical property. The proposed method is not intended to replace detailed numerical modeling but to complement it. By providing physically consistent first-order estimates and insight into the governing mechanisms, it enhances design awareness and supports the development of robust lining solutions for tunnels in squeezing ground.

References

Barla G. (2001) Tunnelling under squeezing rock conditions. Rivista Italiana di Geotecnica 35 (4), 38–58.

Barla G., Bonini M., Semeraro M. (2011) Analysis of the behaviour of yield-control support system in squeezing rock. Tunnelling and Underground Space Technology 26 (1), 146–154.

Batocchioni L, González V, Miliziano S. (2024) The effect of a frictional interface in a preliminary yielding support for a deep tunnel. Tunnelling for a Better Life –Proceedings of the ITA-AITES World Tunnel Congress, WTC 2024, 918–931.

Batocchioni L. (2025) Numerical modeling of yielding linings in squeezing conditions. Phd Thesis, Sapienza University of Rome.

Batocchioni L., Turrini E., Pandolfi C., Miliziano S. (2026). An innovative predictive approach for axial force and bending moment estimation in elasto-plastic tunnel linings. Proceedings of CNRIG 2026, L'Aquila, Italy (in press).

Bonini M., Barla G. (2012) The Saint Martin La Porte access adit (Lyon–Turin Base Tunnel) revisited. Tunnelling and underground space technology, 30, 38-54.

Hoek E. (2001) Big tunnels in bad rock. Journal of Geotechnical and Geoenvironmental Engineering 127 (9), 726–740.

Kovàri K. (1998) Tunnelling in squeezing rock. Tunnel 98 (5), 12–31.

Moritz B. (2011) Yielding elements requirements, overview and comparison. Geomechanics and Tunnelling 4 (3), 221–236.

Panet M. (1995) Le calcul des tunnels par la methode convergence-confinement.

Radončić N., Shubert W., Moritz B. (2009) Ductile support design. Geomechanics and Tunnelling, 2(5), 561-577.

Tian H., Chen W., Yang D., Wu G., Tan X. (2016) Numerical analysis on the interaction of shotcrete liner with rock for yielding supports. Tunnelling and Under-ground Space Technology 54, 20–8.

Yang K., Yan Q., Shi Z., Zhang C., Ma S. (2023) Numerical study on the mechanical behavior of shotcrete lining with yielding support in large deformation tunnel. Rock Mechanics and Rock Engineering 56 (2), 1563–1584.